Shear Wave Velocity To Evaluate *In-Situ* State Of Cohesionless Soils

J.C. Cunning[1], P.K. Robertson[2] and D.C. Sego[2]

[1]Golder Associates Ltd.
500-4260-Still Creek Drive
Burnaby, BC
CANADA, V5C 6C6

Tel: (604) 298-6623
Fax: (604) 298-5253

[2]Geotechnical Group
Department of Civil Engineering
220 Civil/Electrical Engineering Building
University of Alberta
Edmonton, Alberta
CANADA, T6G 2G7

Tel: (403) 492-5106
Fax: (403) 492-8198

Submitted to the

Canadian Geotechnical Journal

June 1994

Shear Wave Velocity To Evaluate *In-Situ* State Of Cohesionless Soils

J.C. Cunning, P.K. Robertson and D.C. Sego

ABSTRACT

Shear wave velocity (V_S) measurements were carried out in a triaxial testing program on three different cohesionless soils. The V_S was measured using bender elements during consolidation and at ultimate steady state. After consolidation the soil samples were loaded in shear under constant strain rate triaxial compression either drained or undrained to determine their ultimate steady or critical state (USS) at large strains. The V_S measurements were used to develop relationships between the void ratio (e), mean normal effective stress (p') and V_S. The shear loading results were expressed within the framework of Critical State Soil Mechanics. The results of the V_S and USS information were combined with the state parameter concept to develop an equation to use field measured V_S to estimate the *in-situ* consolidation state within a soil. Thus the contractive/dilative boundary with respect to vertical effective stress for large strain loading can be determined from *in-situ* measurements of V_S. These can then be used as a design aid to determine if a soil deposit is potentially susceptible to flow liquefaction. Worked examples to illustrate the procedure are given.

Key words: Shear wave velocity, cohesionless soil, *in-situ* state, state parameter, liquefaction, laboratory testing

INTRODUCTION

Cohesionless soils can exist in both natural and man made deposits. Geotechnical evaluation of slopes or foundations on these deposits requires investigation into the mechanical behaviour for various static and dynamic loading conditions. This evaluation requires a knowledge of the *in-situ* state of the soil deposit defined by the combination of the void ratio and the effective stress conditions. It is the location of this state relative to the ultimate steady or critical state that provides an estimate of the large strain behaviour of the soil. For any deposit the evaluation of *in-situ* state can be undertaken by either obtaining undisturbed samples of the soil for laboratory testing, or by performing *in-situ* tests.

High quality undisturbed samples of cohesionless soils can be difficult and expensive to obtain. Ground freezing is one method to obtain the highest quality samples available (Sego *et al.* 1994; Yoshimi *et al.* 1989). However, due to the high cost associated with obtaining these undisturbed samples, this approach has been reserved for large budget engineering projects. Laboratory tests can be carried out on reconstituted samples of cohesionless soils. However, the selection of appropriate density and preparation method may influence the measured steady state results (Mulilis *et al.* 1977).

The two primary *in-situ* tests for cohesionless soils are the Standard Penetration Test (SPT) and the Cone Penetration Test (CPT). Other more advanced *in-situ* testing can involve the measurement of shear wave velocity (V_S), resulting in a profile of V_S with depth. Numerous empirical correlations exist to estimate the *in-situ* state of cohesionless soils from penetration test results. Many of these are based on relative density and are strongly influenced by soil compressibility (Robertson and Campanella 1983). There are also empirical correlations to evaluate the potential for liquefaction susceptibility from the SPT blow count (N) (Seed, 1979) or from the CPT tip resistance (q_c) (Robertson *et al.* 1992b). However, there is limited information on the use of V_S for the evaluation of *in-situ*

state and liquefaction susceptibility of a soil. The V_S measured *in-situ* can be compared to a limited historical data base where V_S was measured at sites where liquefaction was or was not reported. A normalized shear wave velocity value of $(V_{S1}) < 160$ m/s was suggested by Robertson *et al.* (1992a) as a value below which the potential for flow liquefaction is high.

This paper describes a method to estimate *in-situ* state of cohesionless soils from the *in-situ* measurement of V_S. This can be accomplished through a laboratory developed relationship between the void ratio (e)- the mean normal effective stress (p') - and the V_S. This interpreted *in-situ* state can be compared to the ultimate steady state (USS) of the soil within the framework of critical state soil mechanics (CSSM). Thus, based on the *in-situ* measured V_S and effective stress condition a prediction can be made about the large strain behaviour of the soil.

For this study a series of monotonic triaxial compression tests, both drained and undrained, with V_S measurement during consolidation and at USS was carried out. The materials tested were Ottawa sand and two tailings sands. The results for Ottawa sand are described in Robertson *et al.* (1994). The tailings sands were an angular tailings sand from a mine in Alaska (Alaska sand) and a subrounded to angular tailings sand from the Syncrude oilsand extraction operation at Fort McMurray, Alberta, (Syncrude sand).

BACKGROUND

According to CSSM concepts a cohesionless soil element exists in a state of void ratio and effective stresses such that it is either loose or dense of USS. A three dimensional space of e, p' and deviator stress (q) can be used to describe boundaries that separate the states at which a soil can or can not exist. When a soil is sheared the void ratio and effective stress move toward an ultimate steady state line (USSL).

A loose cohesionless soil loaded in shear will contract to reach USS and a dense soil will dilate to USS, both independent of the type of loading. Loose cohesionless soils can produce large deformations and thus can be more critical for design. Dense cohesionless soils are typically not a design problem as they will generally not exhibit large deformations upon most loading conditions. Thus the investigation of cohesionless soils is often directed toward quantifying how loose the soil deposit is *in-situ*. When a cohesionless soil is loose of USS and is sheared undrained it tends to contract and pore pressures can increase which can result in strain softening behaviour. The soil can reach a peak strength but then strain soften rapidly to steady state or residual strength. At this steady state there is a state of constant void ratio, effective mean normal stress and shear stress (Castro 1969).

If a natural or man made slope consisting of a loose strain softening cohesionless soil exists in a condition such that the *in-situ* static shear stresses are greater than the ultimate steady state strength, catastrophic collapse and flow liquefaction can occur if the strain softening response is triggered (Robertson 1994). The loading condition to trigger the strain softening response can be either undrained loading such as from an earthquake or drained loading such as the slow rising of the water table (Sasitharan *et al.* 1994). An engineering evaluation into the stability of such a slope would involve evaluating how much of the entire soil profile is susceptible to collapse and hence flow liquefaction.

Much research into the behaviour of loose sands has taken place for both conditions of static and dynamic loading. Most current practice for the evaluation of the susceptibility of a soil to flow liquefaction is based on *in-situ* penetration tests, such as the SPT or CPT.

With the SPT the evaluation is carried out by comparing the measured N to a historical data base of information at sites that have or have not liquefied under past earthquake loading. In order to apply these data base values to all ground conditions,

general correction factors have been developed (Seed 1979), including a correction based on fines content.

Been and Jefferies (1986) suggested using normalized CPT penetration resistance to estimate the *in-situ* state of a sand. This approach requires results from large calibration chamber testing, which are very expensive and are subject to boundary size effects and corrections. In addition, there is uncertainty over the normalization procedure for penetration resistance (Sladen 1989) and extrapolation into the loose range. These *in-situ* penetration tests can provide an estimate of whether the soil is either loose of critical state and therefore contractive, or dense of critical state and dilative. A major disadvantage for the interpretation of penetration tests in cohesionless soils is the uncertainty due to variations in soil compressibility (Robertson and Campanella 1983).

Been and Jefferies (1985) introduced the state parameter (Ψ) to describe the large strain behaviour of a sand based on the combined influence of the initial void ratio, effective confining stress and their relation to the steady state void ratio at the same stress. Been and Jefferies (1985) showed that the initial state of a sand controlled the large strain behaviour.

SHEAR WAVE VELOCITY TO EVALUATE IN-SITU STATE

Robertson *et al.* (1994) have shown that the shear wave velocity (V_S) can be used to estimate the *in-situ* state for Ottawa sand. Shear wave velocity is an attractive parameter since it can be easily measured in both the field and the laboratory. No corrections are required for boundary effects and the normalization procedure for overburden stress is developed directly.

Shear wave velocity is predominantly a function of the void ratio and effective stress conditions in the soil. Soil compressibility, which can have a large effect on SPT and CPT penetration resistance, has little or no effect on shear wave velocity. Fabric, aging and cementation of the soil can also have an affect on shear wave velocity. However, one of the objectives of this study is to estimate the *in-situ* state of sands which may be subject to flow liquefaction. Such sands are likely young and uncemented thus, aging and cementation are unlikely to be of major concern. Fabric can also influence V_S, however, there is evidence to suggest that fabric has little effect in very loose sands (Robertson *et al.* 1994).

State parameter (ψ), as defined by Been and Jefferies (1985) is the difference between the current void ratio and the void ratio of the point on the ultimate steady state line (USSL) with the same mean normal effective stress (p') as the current point. The latter can be defined as follows:

$$e_{ss} = \Gamma - \lambda_{ln} \bullet ln\ (p') \qquad [1]$$

where:

Γ = intercept of USSL at p' = 1 kPa

λ_{ln} = slope of USSL in e-lnp' space

Sasitharan (1994) and Robertson *et al.* (1994) showed that the current void ratio can be estimated by measuring shear wave velocity and using the relationship:

$$e = \frac{A}{B} - \frac{V_S\ (P_a)^{(na + nb)}}{B(\sigma'_a)^{na}(\sigma'_p)^{nb}} \qquad [2]$$

where:

V_S = shear wave velocity, in m/s

σ'_a = the effective stress in the direction of wave propagation, in kPa

σ'_p = the effective stress in the direction of particle motion, in kPa

A and B = constants for a given sand, both in m/s

na and nb = stress exponents; typically, na = nb = 0.125

P_a = atmospheric stress, typically 100 kPa.

Combining equations 1 and 2 with the definition of state parameter (ψ) results in the following equation for state parameter, as given by Sasitharan (1994):

$$\Psi = C - V_{s\Psi} \qquad [3]$$

where:

$$C = \frac{A}{B} - \Gamma \qquad [4]$$

$$V_{s\Psi} = \left(\frac{V_s (P_a)^{na+nb}}{B (\sigma_a')^{na} (\sigma_p')^{nb}} - \lambda_{ln} \, ln \, p' \right) \qquad [5]$$

Making the following substitutions:

$$\sigma_a' = \sigma_h' = K_o \bullet \sigma_v' \qquad [6]$$

$$\sigma_p' = \sigma_v' \qquad [7]$$

$$p' = \frac{1}{3}(\sigma_1' + 2\sigma_3') = \frac{1}{3}(\sigma_v' + 2\sigma_h') = \frac{\sigma_v'}{3}(1 + 2K_o) \qquad [8]$$

results in the following equation relating state parameter to shear wave velocity:

$$\Psi = \left(\frac{A}{B} - \Gamma \right) - \left(\frac{V_s (P_a)^{na+nb}}{B (\sigma_v')^{na+nb} (K_o)^{na}} - \lambda_{ln} \, ln \left[\frac{\sigma_v'}{3}(1 + 2K_o) \right] \right) \qquad [9]$$

From this equation, it can be seen that state parameter is a function of soil type (A, B, Γ and λ_{ln}), K_o, and shear wave velocity, V_s.

Measured values of shear wave velocity, V_s, are usually corrected to a normalized shear wave velocity, V_{s1}, to account for overburden stress, using the following equation:

$$V_{s1} = V_s \left(\frac{P_a}{\sigma_v'}\right)^{na} \cdot \left(\frac{P_a}{\sigma_h'}\right)^{nb} \qquad [10]$$

where P_a = 100 kPa and na = nb = 0.125, typically

Substituting equation 10 into equation 9 results in the following equation relating state parameter to V_{s1}:

$$\Psi = \left(\frac{A}{B} - \Gamma\right) - \left(\frac{V_{s1}}{B\ (K_o)^{na}} - \lambda_{ln}\ ln\left[\frac{\sigma_v'}{3}(1 + 2K_o)\right]\right) \qquad [11]$$

Combining equations 2 and 10 provides a relationship between normalized shear wave velocity, V_{s1}, and void ratio, e:

$$V_{s1} = A - Be \qquad [12]$$

TESTING PROGRAM

A laboratory testing program was carried out to determine the parameters in equation 11. The modified triaxial testing equipment use for this study is described in detail by Robertson *et al.* (1994) and Cunning (1994). The main modification of the triaxial cell is the incorporation of bender elements in the load head and base of the cell for the measurement of V_s. Sample preparation was achieved predominantly using the moist

tamping method although water and air pluviation was used for some samples to achieve lower void ratios. V_S was measured with bender elements and travel time of the shear wave was chosen from the oscilloscope using a first pulse arrival technique.

In this research three different cohesionless soil materials were tested. The materials were Ottawa sand (OS), Alaska sand (AS), and Syncrude sand (SS). Grain size distribution curves for these three sands are shown in Figure 1. Ottawa sand is C109 sand from Ottawa, Illinois and is a uniformly graded, rounded to sub rounded, clean quartz sand with a specific gravity of 2.67 and maximum and minimum void ratio of 0.82 and 0.50, respectively using ASTM D2049. The mean grain size, $D_{50} = 0.35$ mm.

Alaska sand is an angular sand obtained from a marine tailings deposit in the state of Alaska. The deposit is from an old mine waste area and has been in a marine environment for up to 70 years. The mean grain size, $D_{50} = 0.12$ mm. The fines content for the Alaska sand was about 32% passing the #200 (74 μm) sieve with a specific gravity of 2.90 and maximum and minimum void ratio of 1.78 and 0.70, respectively using ASTM D2049. The ASTM standard suggests that this method is not reliable for material with a fines content of greater than 5% and thus the maximum and minimum void ratio values are approximate. The fines in the Alaska sand are composed of a large amount of carbonate shell fragements which increases the compressibility of the sand significantly.

Reconstituted tests on Syncrude sand were performed with material obtained as a bulk sample from the beach material at the Syncrude tailings facility. Syncrude sand is a sub angular uniform tailings sand. The Syncrude sand is a tailings by-product of the extraction of oil from the Alberta oilsands. The mean grain size, $D_{50} = 0.17$ mm. The average fines content for the material tested in this research was 12.4% passing the #200 (74 μm) sieve with a specific gravity of 2.62 and maximum and minimum void ratio of 0.96 and 0.52, respectively using ASTM D2049.

RESULTS

Due to limited space, only the result for the Syncrude sand tests will be presented in detail. The results for Ottawa sand have been presented in detail by Robertson *et al.* (1994). The Alaska sand results are presented in detail by Cunning (1994).

A total of 10 tests were carried out on the Syncrude sand. Nine of the 10 test samples were prepared by the moist tamping technique and 1 sample was prepared using the air pluviation technique. All samples were isotropically consolidated to between 54 and 453 kPa effective confining stress with V_S measurement made throughout consolidation. After consolidation seven of the samples were sheared undrained and four were sheared drained using a constant strain rate of 0.15 mm/min until the ultimate steady state condition was achieved.

Figure 2 shows the Syncrude sand consolidation data in terms of V_S against e and V_S against the mean normal effective consolidation stress p'c. In Figure 2a it can be seen that three ranges of void ratio were obtained for the Syncrude sand. The range where most of the data exists is for the moist tamped samples prepared with an initial 5% moisture content and to create very loose samples. For a slightly denser sample one test was moist tamped at 10% moisture content. While for the densest sample tested the technique of air pluviation was used to prepare the sample.

Figures 2a and 2b show that the V_S is changing with both the e and p'c. Figure 2b includes lines of constant e predicted by equation (2) for Syncrude sand. A slight deviation of the data from the line of constant e is expected since Syncrude sand has a very low compressibility and e changes slightly during consolidation. In order to compare the data, V_S was normalized with p'c using equation (10) with an exponent of na + nb = n = 0.26. The exponent value of 0.26 was chosen from the best fit linear regression through the experimental data. Figure 3 shows the values of normalized shear wave velocity V_{S1}

against void ratio for Syncrude sand during isotropic consolidation. The average Syncrude sand V_{s1} - e equation was determined from linear regression and can be expressed as;

$$V_{s1} = 311 - 188\ e \qquad [13]$$

with upper and lower bounds to all the data expressed by the equation as;

$$V_{s1}\ \text{upper} = 321 - 118\ e \qquad [14]$$

$$V_{s1}\ \text{lower} = 302 - 188\ e \qquad [15]$$

The average Syncrude sand equation (13) for V_{s1} versus e was combined with the normalization equation (10) to give the average e-p'c-V_s equation as;

$$V_s = \{311-(188xe)\} \times (p'c/100)^{0.26} \qquad [16]$$

This equation was used to develop contours shown on a plot of e against log p' (Figure 4). Also shown on Figure 4 are some of the consolidation data for Syncrude sand and the USSL derived from shear loading tests that are described in a later section. Figure 4 shows that Syncrude sand has a low compressibility reflected in the small change in void ratio during consolidation. Each consolidation state is marked with its laboratory measured V_s and good agreement to the contours can be noted.

After consolidation all samples were then loaded in shear either undrained or drained and the USS parameters for Syncrude sand determined. As a part of the Canadian Liquefaction Experiment, (CANLEX) project testing by other university laboratories was carried out on similar bulk samples of Syncrude sand. Tests at the University of British Columbia (UBC) were prepared using both water pluviation (WP) and air pluviation (AP). Tests at the Centre for Cold Oceans Resources Engineering (C-CORE) were prepared by air pluviation (AP). All tests at the other laboratories were undrained and some were carried out using triaxial compression, triaxial extension and simple shear. The results of

the undrained and drained triaxial compression tests from this study along with selected test results from the other laboratories are shown together in Figure 5 in a plot of e against log p'.

When samples were sheared to ultimate steady state, shear wave velocity measurements were made. The normalized shear wave velocity values at ultimate steady state are compared to the V_{s1} - e relationship based on the isotropic consolidation states in Figure 6. The V_{s1} values at USS are similar to those during isotropic consolidation. Figure 6 indicates that the reslationship between V_s, e and p' appears to fit isotropic consolidation states as well as anisotropic stress states at USS. This suggests that fabric plays a minor role in this relationship, since the fabrc at USS will be different than that during isotropic consolidation.

Figure 7a shows the normalized stress paths for the undrained tests from this study for Syncrude sand. The stresses are normalized by the mean effective normal stress at the ultimate steady state (p'uss) for the given void ratio. The USS point can be seen as well as the clearly defined collapse surface from the undrained tests. The slope of the collapse surface is s = 0.9 taken through the USS point and is similar to the collapse surface of s = 0.8 for Ottawa sand (Sasitharan *et al.* 1994)

Figure 7b shows an expanded view of the USS point and the collapse line. Also shown are the normalized stress paths for the drained tests from this study which all rise up from a low value of p'/p'uss to the USS point of (1, M). Because they start at a low value of p'/p'uss they do not plot clearly as individual tests on the normalized stress path. The collapse surface can be seen to occur at a mobilized friction angle less than the USSL.

From all the data in Figures 5 and 7 the following USS parameters were determined for Syncrude sand.

$$\Gamma = 0.928$$

$\lambda_{In} = 0.0277$

$M = 1.31$ ($\phi'm = 32.5°$)

These values are valid over a stress range of p' = 6 to 800 kPa.

The results of all three different cohesionless materials are summarized in Table 1 for their V_S parameters, (A, B and n) and their USS parameters (Γ, λ_{In}, M). It should be noted that the USS parameters for Alaska sand are very different from those of Ottawa and Syncrude sand. The Alaska sand is considerably more compressible than the other sands, due primarily to the highly crushable carbonate shell fragements within the fines. Fear and Robertson (1994) noted that the USS parameters for Alaska and Ottawa sand appear to bound most sands.

Figure 8 presents a summary of the V_S measurements during consolidation for all three sands in terms of normalized shear wave velocity versus void ratio. Although each data set has different values for A and B, the complete data set is remarkably consistent. If an average relationship between V_{S1} and e is developed for all the sands the resulting constants are A = 359 B = 231. The consistency in the data set is in general agreement with previous work (e.g. Hardin and Richard, 1963) and illustrates how the shear wave velocity is controlled predominantly by void ratio and effective confining stress.

ANALYSIS

The state parameter based on shear wave velocity for each sand can be evaluated using the soil constants, A, B, Γ, and λ_{In} from Table 1 and equation 11. However, the first concern when applying the sand specific equations of e-p'-V_S with the USS parameters is to evaluate the effect of the previously determined upper and lower bounds of

this relationship on the boundary. The effects of the scatter in the e-p'-V_S relation is investigated in Figure 9 which shows the contractive/dilative boundary ($\Psi = 0$) for the Syncrude sand for $K_O = 0.4$ based on the average, upper and lower bound of the e-p'-V_S equation. The range in the contractive/dilative boundary is about 8 m/s for Syncrude sand at σ'_V = 100 kPa stress level for a $K_O = 0.4$. This variation increases slightly with increasing σ'_V.

Since the relationships have been developed based on the mean effective stress (p'), K_O has an influence. Figure 10 show the V_S - σ'_V relationship for the average sand specific e-p'-V_S equation for the case of K_O = 0.4 and K_O = 1.0 for the Syncrude sand. The difference is approximately 25 m/s at σ'_V of 100 kPa. This difference increases slowly as σ'_V increases. For a high K_O in a deposit, a higher V_S value is required for the soil to remain on the dilative side of USS.

Figure 11 shows the average contractive/dilative boundary for the three sands tested in this study in terms of V_S against σ'_V for a $K_O = 0.4$ using the parameters summarized in Table 1. It is interesting to note that the $\Psi = 0$ boundaries are not vastly different even though the USSL for Alaska sand is very different from those of Ottawa and Syncrude sand.

The values of the parameters in Table 1 combined with equation 11 can be used to evaluate the state parameter (ψ) for each of the three tested soils based on *in-situ* values of shear wave velocity. Ottawa sand is representative of a clean, uniform silica sand. Syncrude sand is representative of a uniform fine sand with some fines. Both sands produce similar relaitonships between V_S and ψ. However, Alaska sand is a highly compressible sand resulting in a slightly flatter relationship between V_S and ψ (see Figure 11).

The relationships shown in Figure 11 have been developed based on reconstituted laboratory samples. Hence, the resulting relationships will only represent young, uncemented cohesionless soil. The *in-situ* material could be aged or cemented and have a different behaviour. Both aging and cementation will tend to increase the measured shear wave velocity. Aging generaly decreases the void ratio of a cohesionless soil and can result in a more dilatant response. Cementation can increase the small strain stiffness of a soil, however when strains are sufficient to break the cementation bonds, the large strain behaviour can be contractant or dilatant depending on the void ratio.

COMPARISON WITH PENETRATION BASED METHODS

Been and Jefferies (1986) suggested using normalized CPT penetration resistance to estimate state parameters. Robertson *et al.* (1992) suggest a correlation between normalized shear wave velocity (V_{s1}) and normalized cone penetration resistance (q_c), as follows;

$$q_{c1} = \left(\frac{V_{s1}}{102}\right)^4 , \text{MPa} \qquad [17]$$

where V_{s1} is in m/s.

If this relationship is applied to the Ottawa sand relation between V_s and ψ, the resulting correlation between q_c and ψ for $K_o = 0.4$ is shown in Figure 12. Also shown in Figure 12 is the Been and Jefferies (1986) correlation for Ottawa Sand. In general, the two correlations are similar. However, the relationship derived from V_s is nonlinear, suggesting that the linear correlation by Been and Jefferies (1986) may be incorrect. This is consistent with the suggestion by Sladen (1989).

Fear and Robertson (1994) showed that the site specific correlation between CPT q_c and V_S for Alaska sand was as follows;

$$q_{c1} = \left(\frac{V_{s1}}{135}\right)^4, \text{ MPa.} \qquad [18]$$

The difference between equation (17) and (18) reflects the increased compressibility of the Alaska sand. Hence, for a given shear wave velocity, the Alaska sand will have a much smaller penetration resistance (q_c) due to the high compressibility.

The resulting relationship between q_c and ψ for Alaska sand derived from the site specific reltaionship in equation 18, is significantly different than that shown in Figure 12 for Ottawa sand. This illustrates the important influence of compressibility on any correlation between penetration resistance and state parameter.

EXAMPLE APPLICATION

Two worked examples will be given where *in-situ* state is estimated to determine if the potential for flow liquefaction exists. The examples will combine site investigation data with the analysis developed from their laboratory test results.

Alaska Sand Example

For this worked example data was used from two soundings with SPT blow count values as well as three seismic cone penetration tests (SCPT) profiles. The five investigation holes were all along a section line in order to analyze the soil profile for possible liquefaction. The stratigraphy of the soil profile consisted of about 15 m of silty sandy tailings material mixed with shell fragments. The lower portion from 15 m to 22 m

consisted of beach sand and silt deposit possibly mixed with tailings material. The field V_s data from the SCPT was in the range of 100 m/s to 250 m/s for a vertical effective stress from 10 to 250 kPa. The σ'_v was calculated based on an estimated bulk soil density of 20 kN/m^3 and with the water table just below the surface.

The *in-situ* measured data are shown on a plot of V_s against σ'_v with the contractive/dilative boundary ($\psi = 0$) in Figure 13. It can be seen that for an assumed K_o of 0.4, all the *in-situ* V_s data plots above the proposed boundary and hence the *in-situ* state is estimated to be on the dilatant side of USS. If the assumed K_o value was increased the boundary would shift toward the data points. It is estimated that for this soil that the *in-situ* K_o is close to the 0.4, but even with an upper bound case of $K_o = 1.0$ almost all the data would still plot above this line on the dilatant side.

Figure 14 shows some of the *in-situ* CPT penetration resistance, q_c data. Also shown is the contractive/dilative ($\Psi = 0$) boundary suggested by Robertson *et al.* (1992b) for a clean, in compressible, uncemented silica sand. The $\Psi = 0$ boundary obtained from this study in terms of V_s for a $K_o = 0.4$ is converted to q_c using the site specific relationship between V_{s1} and q_{c1} (equation 18), and is also shown on Figure 14. It can be noted that the field q_c data plots well above the $\Psi = 0$ boundary defined in this study and below the $\Psi = 0$ boundary for the incompressible silica sand. CPT q_c data interpretation using the conventional incompressible sand correlations appears to be in error due to the high compressibility of the Alaska sand. The measured q_c is found to be lower than values given for an incompressible sand. Thus, applying the typical empirical correlations for CPT can result in an evaluation that suggests that the material is loose of USS. Based on the *in-situ* V_s measurements and the laboratory test result, this conclusion would be extremely conservative for this sand.

It is also important to note that the samples of Alaska sand prepared in the laboratory that were loose of USS and when sheared undrained were highly contractant but did not

strain soften. Thus, these samples were not collapsible and hence, not susceptible to flow liquefaction. It is also worth noting that if the slope of the steady state line ($\lambda_{\ell n}$) was applied to the method proposed by Been and Jefferies (1986) a similar relationship between cone resistance (q_c) and σ'_v would also be obtained ($\psi = 0$ for $q_c \approx 0.9\ \sigma'_v$).

Syncrude Sand Example

As part of the CANLEX project a very detailed site investigation has been undertaken at the site of the Syncrude Settling Basin. This tailings structure is in excess of 40 meters high. SCPT data was obtained at the site between a depth of 27 meters to 37 meters. This zone was the main interest for the CANLEX investigation. The vertical effective stress σ'_v was calculated based on bulk soil density data from geophysical logs and the measured water table which was at a depth of 20 m. The *in-situ* V_s data are plotted against σ'_v showing the proposed contractive/dilative boundary ($\psi = 0$) for Syncrude sand in Figure 15. The boundary shown was developed in this study for the case of $K_o = 0.5$ and $K_o = 0.8$ which represent the estimated range of K_o at the depth considered for the Syncrude field data. It can be seen that the data plots close to the contractive/dilative boundaries.

Based on high quality geophysical logs and high quality undisturbed samples obtained using *in-situ* freezing (Hofmann *et al.*, 1994) the soil within the zone shown in Figure 15 is considered to be close to the contractant/dilatant boundary. Hence, the proposed boundary based on shear wave velocity for Syncrude sand appears to agree with the other in-situ data. Testing of the undisturbed samples is currently underway and results will be published shortly.

CONCLUSIONS

Bender element technology was successfully used to measure the shear wave velocity (V_S) in triaxial testing of loose cohesionless soils. The material tested included a uniform clean quartz sand, and two tailings sands one with 12% and the other with 32% fines passing the #200 sieve (75 μm). The V_S data obtained during consolidation was used to develop sand specific e-p'-V_S relationships. Shear loading was carried out on most of the samples and the results were used to determine the ultimate steady state (USS) parameters. These parameters are based on tests conducted in this research as well as some results by others on Ottawa and Syncrude sand associated with the CANLEX Project. These USS parameters are representative of the reconstituted samples taken to large strains.

Based on the relationship between void ratio, effective confining stress and shear wave velocity plus the equation for the ultimate steady state line, the *in-situ* state of the sand can be estimated. Hence, the contractive/dilative behaviour of a sand can be evaluated from *in-situ* shear wave velocity and vertical effective stress with an estimate of K_o.

The relationships developed in this study are for uncemented, freshly deposited Ottawa, Syncrude and Alaska sands. These sands encompass a wide range of cohesionless soils. Hence, the procedures developed in this study can be applied to a wide range of soils. For aged or cemented soils, the procedures and resulting relationships based on freshly deposited, reconstituted samples may not be valid. However, frequently it is the young, uncemented sand deposits that represent the highest risk of flow liquefaction. The *in-situ* measurment of both shear wave velocity and penetration resistance using the seismic cone pentrative test represents a potential means to identify unusual cohesionless soils that may be aged, cemented or highly compressible.

The proposed procedure and relationship to estimate *in-situ* state (Ψ) based on shear wave velocity measurements has the advantage that the shear wave velocity measurement is

independent of soil compressibility, unlike penetration test results. The relationship involves a normalization for overburden stress that is developed based on laboratory results that does not involve any prior assumptions or corrections for boundary size effects.

ACKNOWLEDGEMENTS

This work was (partly) supported by CANLEX (Canadian Liquefaction Experiment), which is a project funded through a Collaborative Research and Development Grant from the Natural Science and Engineering Research Council of Canada (NSERC), B.C. Hydro, Quebec Hydro, Syncrude Canada Ltd. and Suncor. The collaboration includes the geotechnical consultants, EBA Engineering Consultants Ltd., HBT AGRA, Klohn-Crippen Ltd., Golder Associates and Thurber Engineering Ltd., as well as faculty and students from the University of Alberta, University of British Columbia, Université of Laval, Carleton University and Sherbrooke University. Steffen, Robertson and Kirsten (Canada) Inc. kindly provided the field data and samples for Alaska sand. The first author would like to acknowledge the financial assistance from his NSERC scholarship.

REFERENCES

Been, K., and Jefferies, M.G. 1985. A state parameter for sands. Geotechnique, **35**(2): 99-112.

Been, K., Crooks, J.H.A., Becker, D.E. and Jefferies, M.G., 1986. The Cone Penetration Test in Sands: Part I, State Parameter Interpretation, Geotechnique, 36(2): 239-249.

Been, K., Jefferies, M. G., and Hachey, J. 1991. The critical state of sands. Geotechnique, **41**(3): 365-381.

Castro, G. 1969. Liquefaction of sands. Harvard Soil Mechanics Series No. 81, Harvard University, Cambridge, MA.

Cunning, J.C. 1994. Shear wave velocity measurement of cohesionless soils for the evaluation of *in-situ* state. M. Sc. thesis, Department of Civil Engineering, University of Alberta, Edmonton, Alberta.

Fear, C. and Robertson, P.K., 1994. Estimating the undrained shear strength of sand: a theoretical framework, Submitted to Canadian Geotechnical Journal.

Hardin, B.O., and Richart, F.E. Jr. 1963. Elastic wave velocities in granular soils. ASCE Journal of the Soil Mechanics and Foundations Division, **89**(SM1): 33-65.

Hofmann, B.A., Sego, D.C. and Robertson, P.K., 1994. Undisturbed sampling of a deep loose sand using Ground Freezing, Submitted to Canadian Geotechnical Journal.

Mulilis, J.P., Seed, B.H., Chan, C.K., Mitchell, J.K., and Arulanandan, K. 1977. Effects of sample preparation on sand liquefaction. ASCE Journal of the Geotechnical Engineering Division, **103**(GT2): 91-108.

Robertson, P.K. 1994. Suggested terminology for liquefaction. 46th Canadian Geotechnical Conference, Halifax.

Robertson, P.K. and Campanella, R.G., 1983. Interpretation of Cone Penetrative Tests: Drained Soils, Canadian Geotechnical Journal.

Robertson, P.K., Woeller, D.J., and Finn, W.D.L. 1992a. Seismic cone penetration test for evaluating liquefaction potential under cyclic loading. Canadian Geotechnical Journal, **29**: 686-695.

Robertson, P.K., Woeller, D.J., Kokan, M., Hunter, J., and Luternauer, J. 1992b. Seismic techniques to evaluate liquefaction potential. 45th. Canadian Geotechnical Conference, Toronto, Ontario, October 26-28, 1992. pp. 5:1-5:9.

Robertson, P.K., Sasitharan, S., Cunning, J.C. and Sego, D.C. 1994. Shear wave velocity to evaluate flow liquefaction. Submitted to the ASCE Journal of Geotechnical Engineering, May 1994.

Roesler, S. K. 1979. Anisotropic shear modulus due to stress anisotropy. ASCE Journal of the Geotechnical Engineering Division, **105**(GT7): 871-880.

Roscoe, K.H., Schofield, A.N., Wroth, C.P. 1958. On the yielding of soils. Geotechnique, **8**: 22-53.

Sasitharan, S. 1994. Collapse behaviour of very loose sand. Ph.D. thesis, Department of Civil Engineering, University of Alberta, Edmonton, Alberta.

Seed, H.B. 1979. Soil liquefaction and cyclic mobility evaluation for level ground during earthquakes. ASCE Journal of the Geotechnical Engineering Division, **105**(GT2): 201-255.

Sego, D.C., Robertson, P.K., Kilpatrick, B.I., and Pillai, V.S. 1994. Ground Freezing and sampling of foundation soils at Duncan Dam. Canadian Geotechnical Journal. (accepted for publication in Duncan Dam Case History, Volume Dec. 1994).

Sladen, 1989. Discussion on Cone Penetration Test Calibration for Erksak (Beaufort Sea) sand, Canadian Geotechnical Journal, **26**: 173-177.

Strachan, P. 1981. An investigation of the correlation between geophysical and dynamic properties of sand. Proceedings, Oceans 1981, pp. 399-403.

Tokimatsu, K., and Hosaka, Y. 1986. Effects of sample disturbance on dynamic properties of sand. Soils and Foundations, **26**(1): 53-64.

Yoshimi, Y., Tokimatsu, K., and Hosaka, Y. 1989. Evaluation of liquefaction resistance of clean sands based on high-quality undisturbed samples. Soils and Foundations, **29**(1): 93-104.

List of Tables

Table 1. Summary of ultimate steady state parameters and shear wave velocity parameters for Ottawa, Alaska and Syncrude sands.

List of Figures

Figure 1. Grain size distribution curves for Ottawa, Alaska and Syncrude sands.

Figure 2 a). Shear wave velocity versus void ratio and b). shear wave velocity versus mean normal effective consolidation stress during isotropic consolidation on Syncrude sand.

Figure 3. Normalized shear wave velocity versus void ratio during isotropic consolidation on Syncrude sand.

Figure 4. Void ratio versus logarithm mean normal effective stress with contours of shear wave velocity in m/s and consolidation data marked with laboratory measured V_s in m/s for Syncrude sand.

Figure 5. Void ratio versus logarithm mean normal effective stress at ultimate steady state for Syncrude sand.

Figure 6. Comparison of the average V_{s1} - e relationship during isotropic consolidation for Syncrude sand with V_{s1} measured at ultimate steady state.

Figure 7. Normalized stress paths for tests on Syncrude sand a). undrained tests with collapse line, b). drained tests, and an expanded view of undrained tests collapsing to USS.

Figure 8. Summary of all test results (Ottawa, Alaska, Syncrude sand) in terms of normalized shear wave velocity versus void ratio.

Figure 9. V_S versus σ'_v with contractive/dilative boundary ($\psi = 0$) for Syncrude sand showing limits of variation of the boundary due to e-p'-V_S variation.

Figure 10. V_S versus σ'_v with contractive/dilative boundary ($\psi = 0$) for Syncrude sand for $K_o = 0.4$ and for $K_o = 1.0$.

Figure 11. V_S versus σ'_v with contractive/dilative boundary ($\psi = 0$) for Ottawa, Alaska and Syncrude sands for $K_o = 0.4$.

Figure 12. Comparison between contours of state parameter using cone penetration resistance, q_c, based on V_S correlation and method proposed by Been and Jefferies (1986) for Ottawa sand ($K_o = 0.4$).

Figure 13. Alaska sand field data in terms of shear wave velocity compared to proposed contractive/dilative boundary.

Figure 14. Alaska sand field CPT qc data versus σ'_v showing the contractive/dilative boundary determined in this study and that suggested by Robertson *et al.* (1992b) for an incompressible clean, silica sand.

Figure 15. Syncrude sand field data in terms of shear wave velocity compared to proposed contractive/dilative boundary.

Table 1. Summary of ultimate steady state parameters and shear wave velocity parameters for Ottawa, Alaska and Syncrude sands.

Material	Fines Content %	Ultimate Steady State Parameter			Shear Wave Velocity Parameters		
		Γ	$\lambda_{\ell n}$	M	A	B	n
Ottawa Sand	0	0.926	0.0324	1.20	381	259	0.26
Alaska Sand	31.7	1.485	0.1172	1.48	307	167	0.26
Syncrude Sand	12.5	0.928	0.027	1.31	311	188	0.26

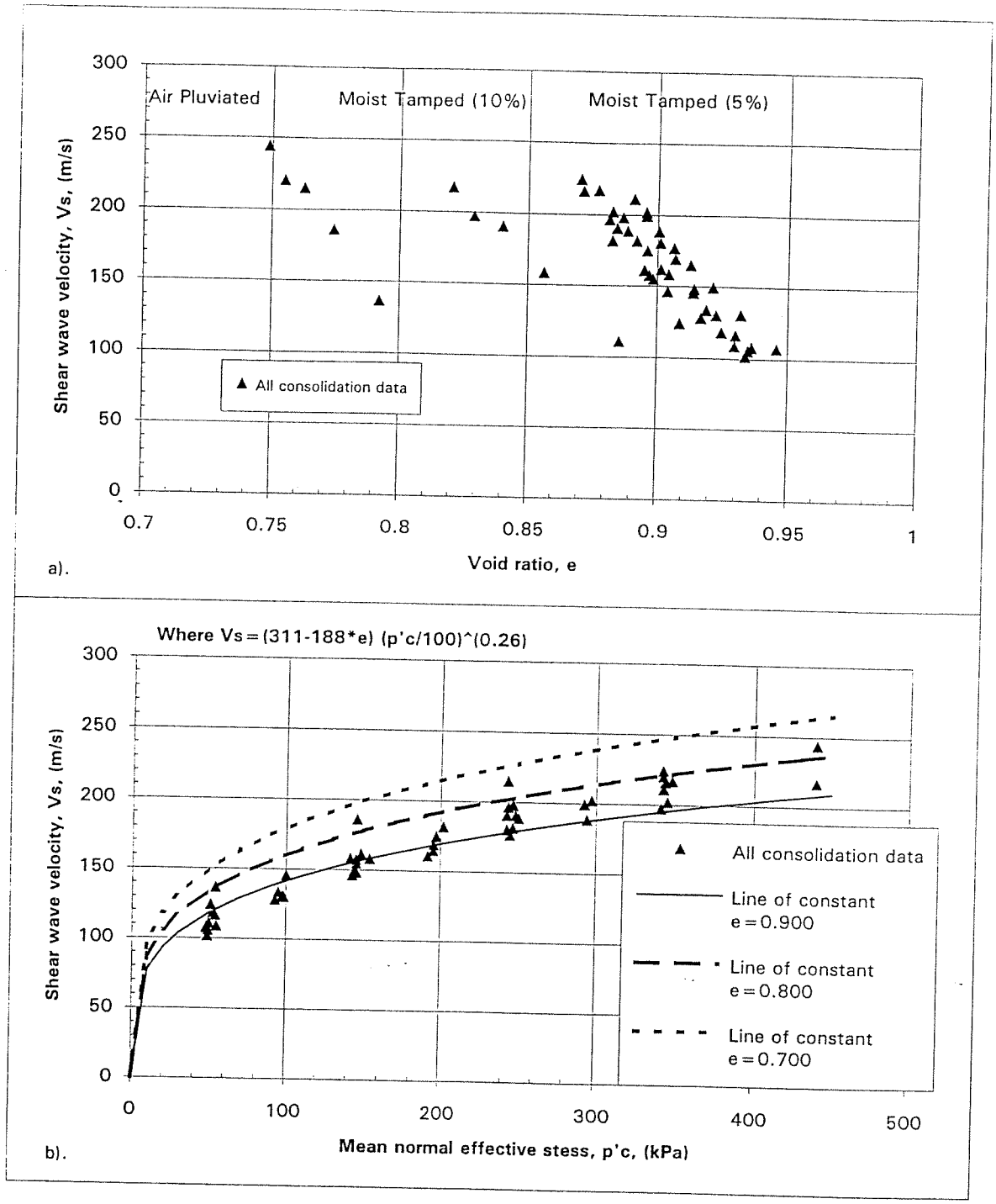

Figure 2 a). Shear wave velocity versus void ratio and b). shear wave velocity versus mean normal effective consolidation stress during isotropic consolidation on Syncrude sand.

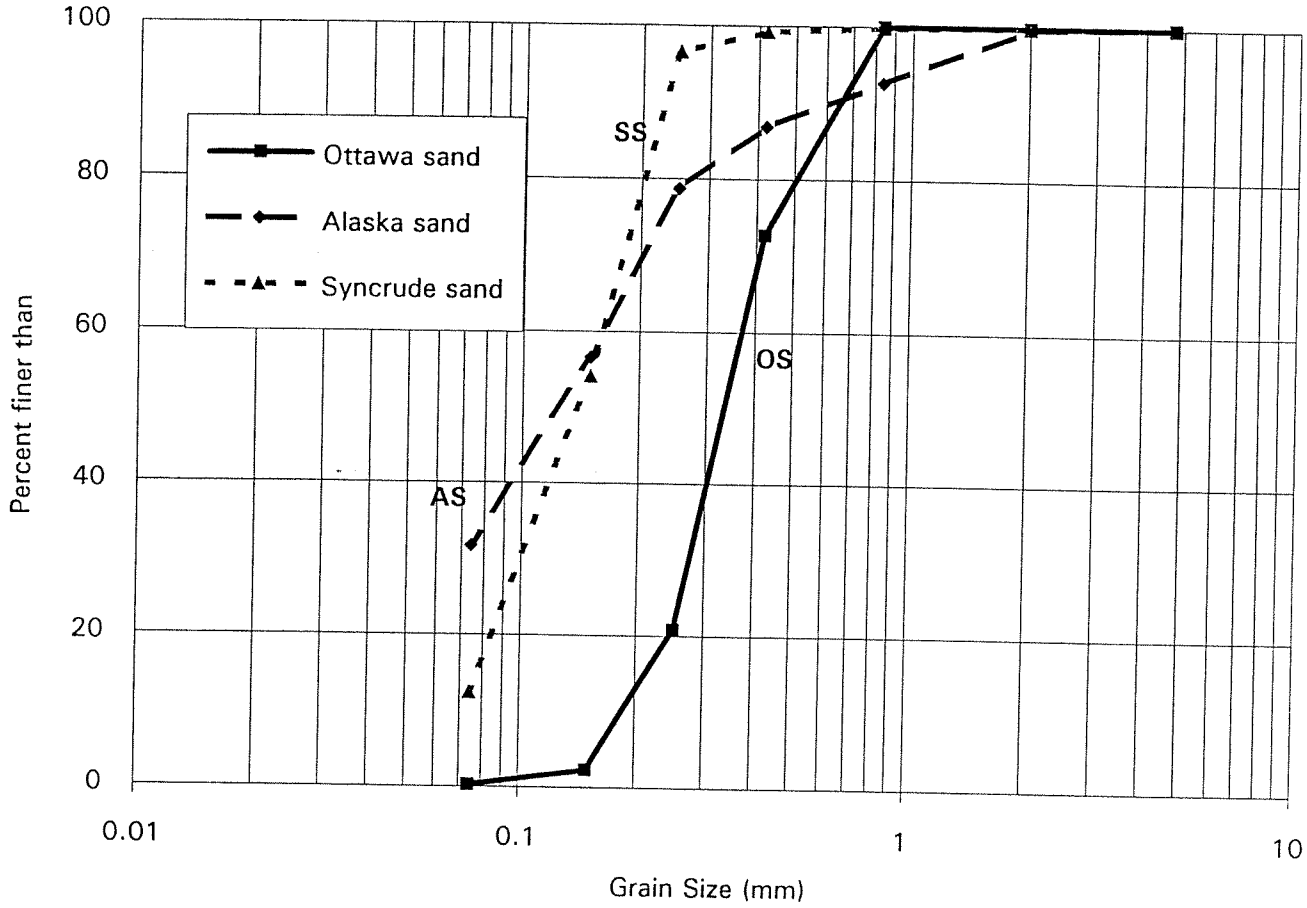

Figure 1. Grain size distribution curves for Ottawa, Alaska and Syncrude sands.

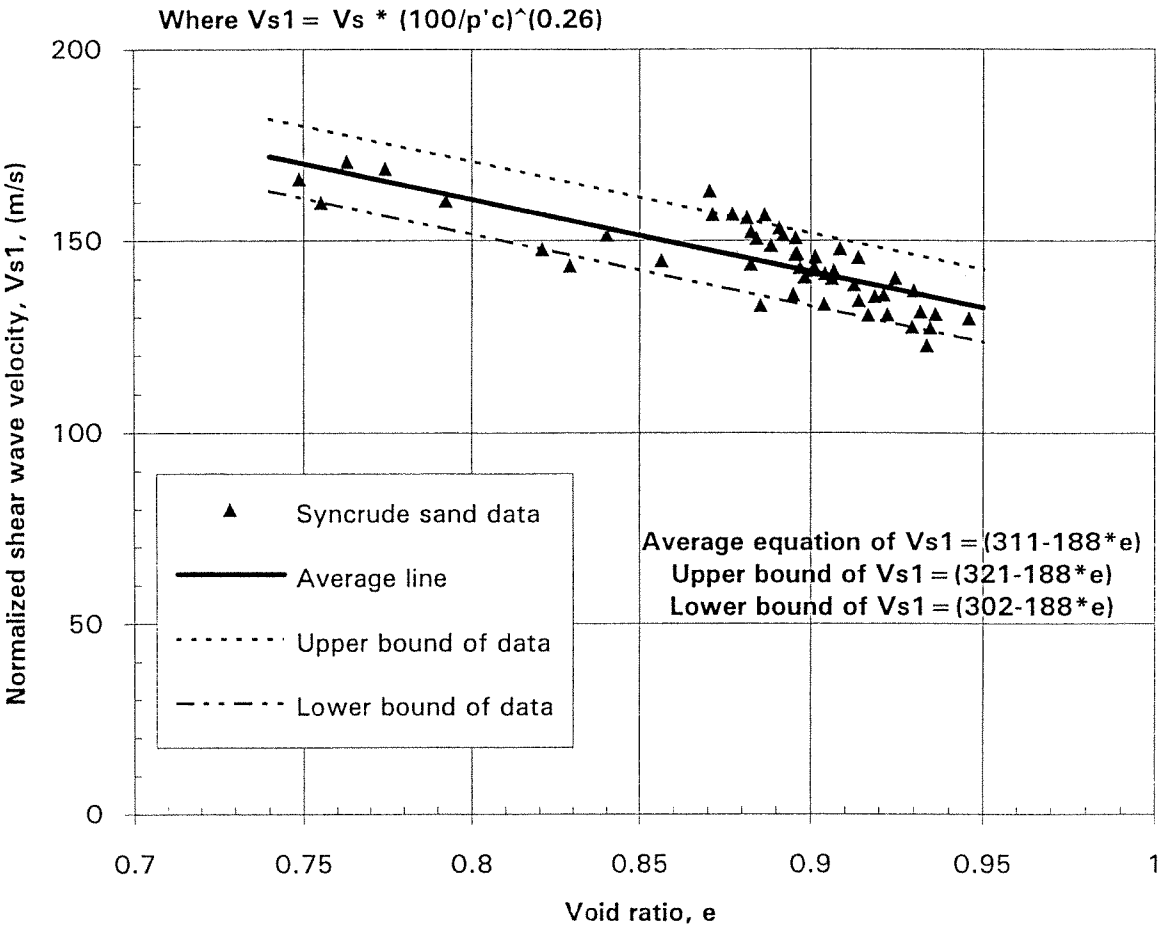

Figure 3. Normalized shear wave velocity versus void ratio during isotropic consolidation on Syncrude sand.

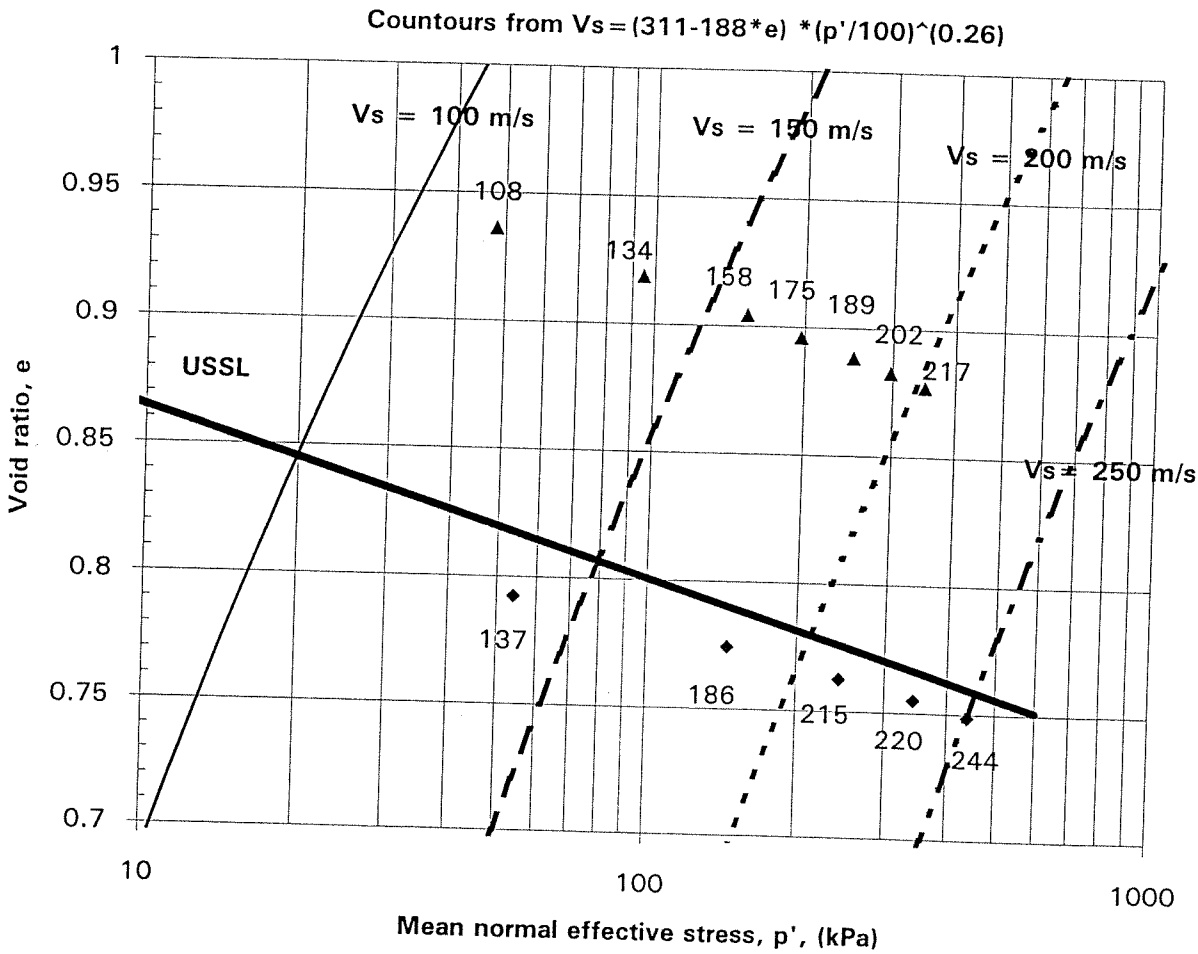

Figure 4. Void ratio versus logarithm mean normal effective stress with contours of shear wave velocity in m/s and consolidation data marked with laboratory measured V_s in m/s for Syncrude sand.

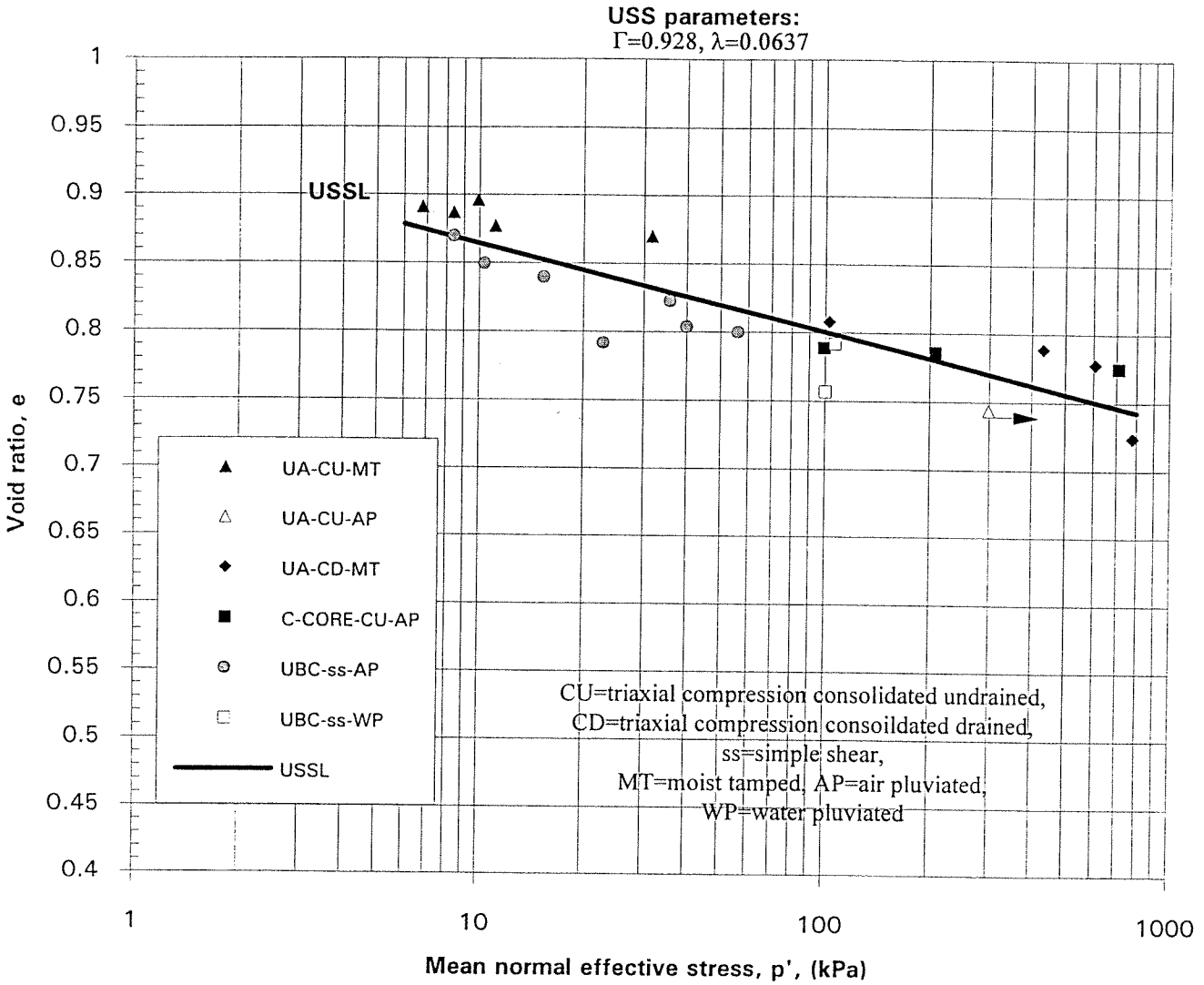

Figure 5. Void ratio versus logarithm mean normal effective stress at ultimate steady state for Syncrude sand.

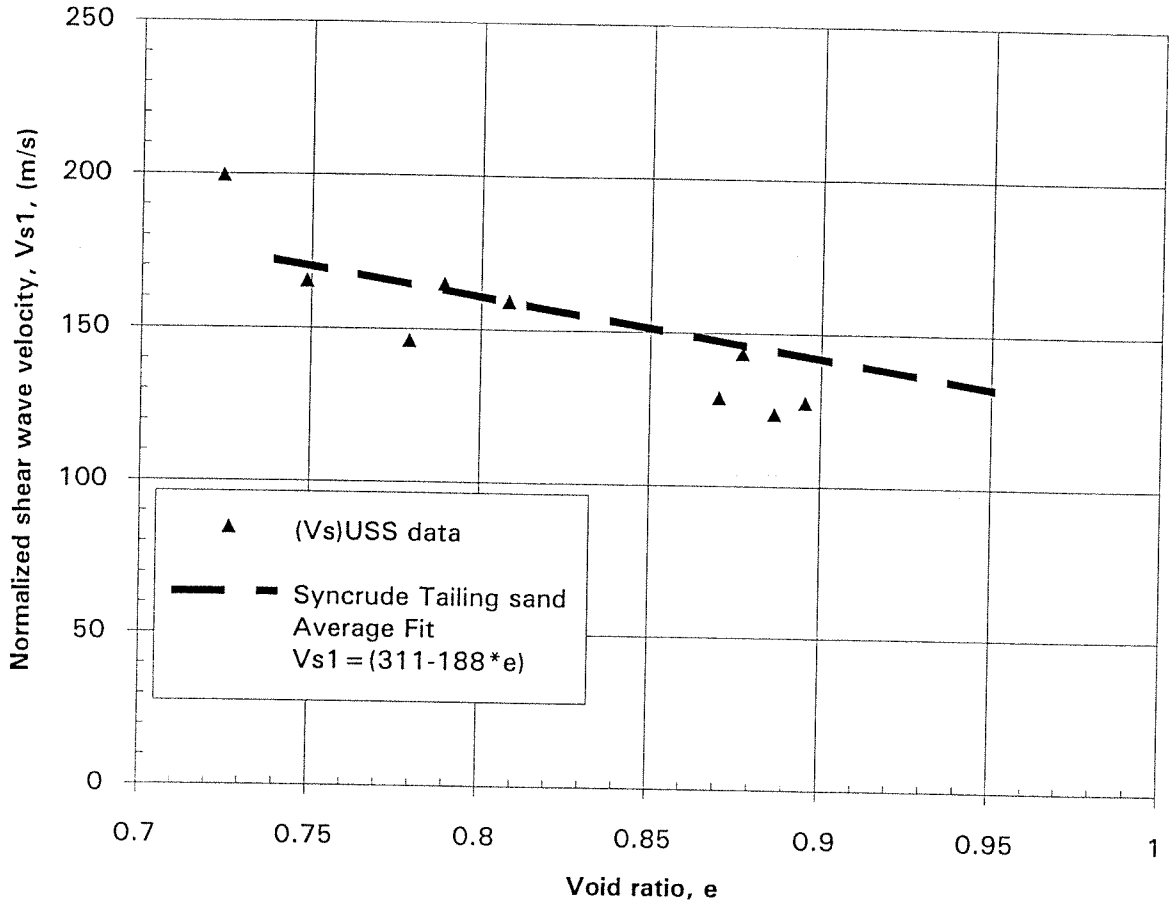

Figure 6. Comparison of the average V_{s1} - e relationship during isotropic consolidation for Syncrude sand with V_{s1} measured at ultimate steady state.

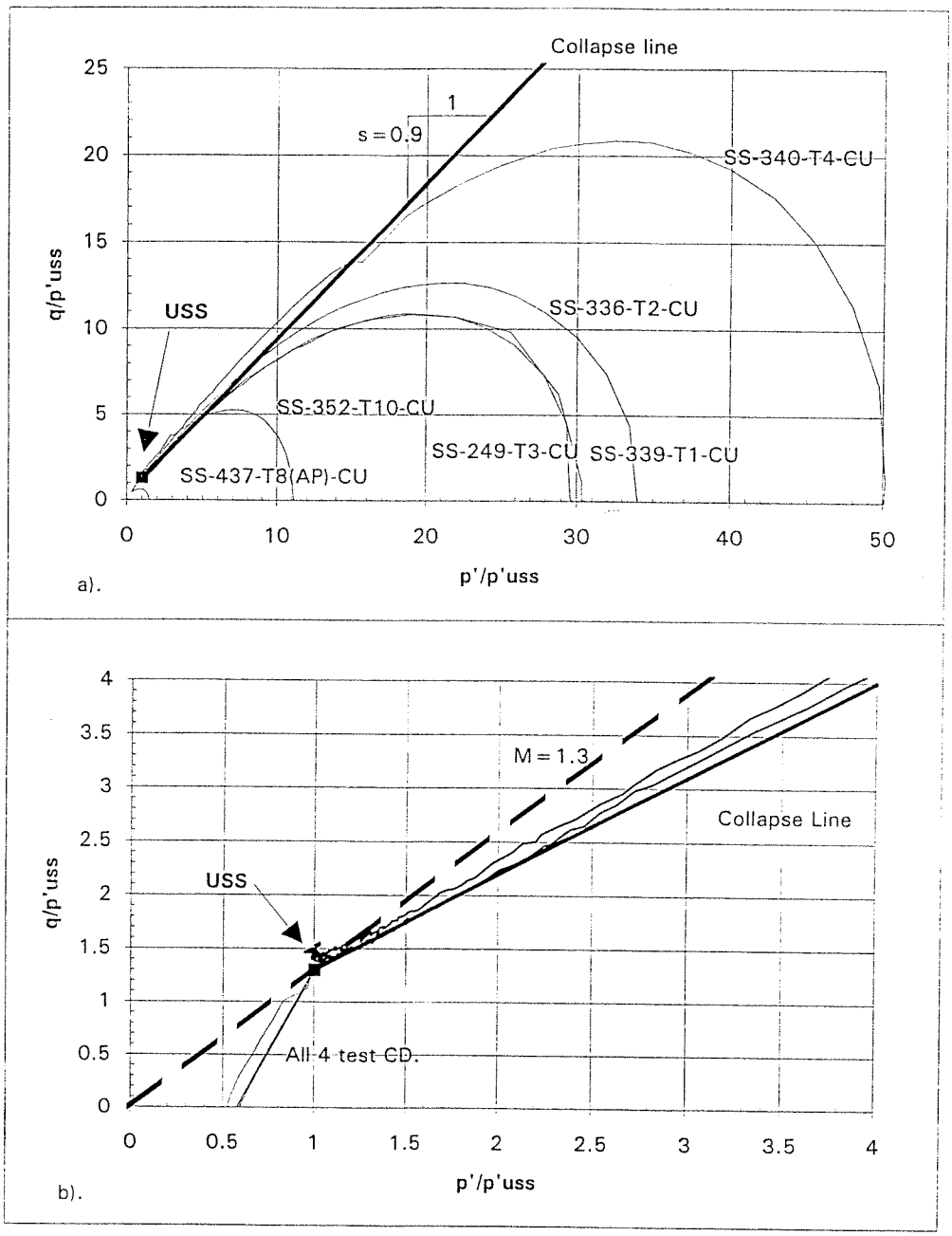

Figure 7. Normalized stress paths for tests on Syncrude sand a). undrained tests with collapse line, b). drained tests, and an expanded view of undrained tests collapsing to USS.

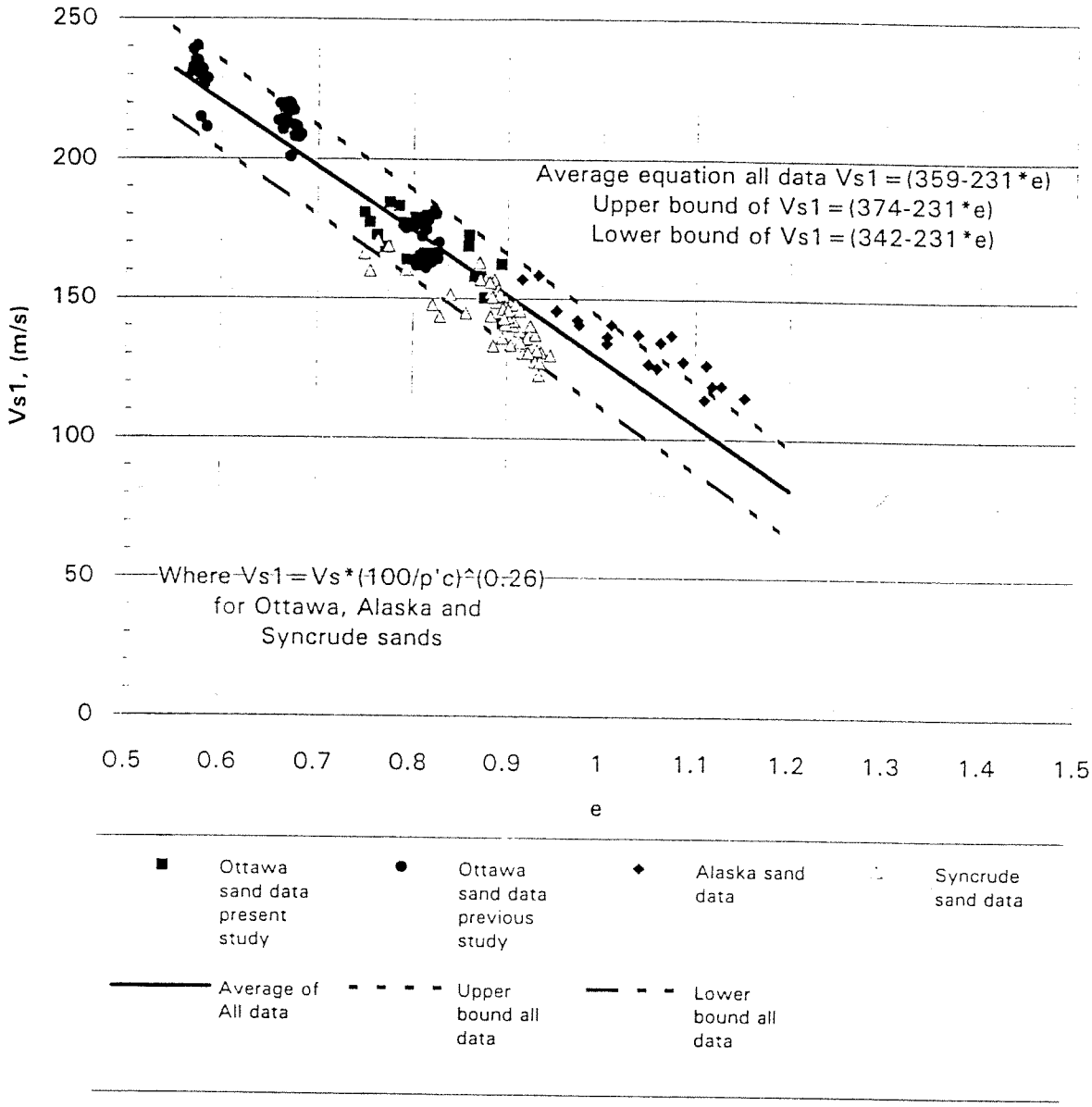

Figure 8. Summary of all test results (Ottawa, Alaska, Syncrude sand) in terms of normalized shear wave velocity versus void ratio.

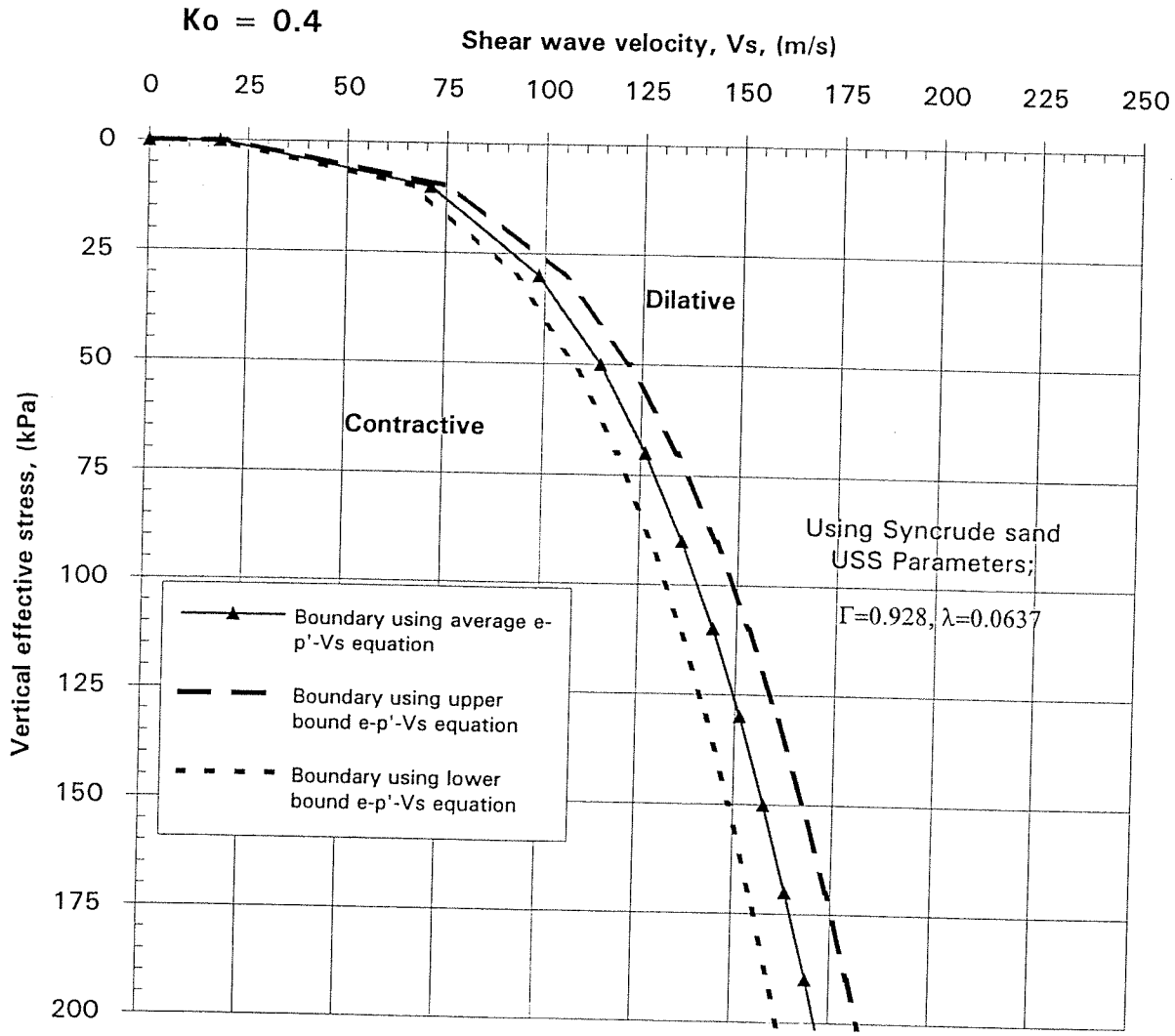

Figure 9. V_S versus σ'_v with contractive/dilative boundary ($\psi = 0$) for Syncrude sand showing limits of variation of the boundary due to e-p'-V_S variation.

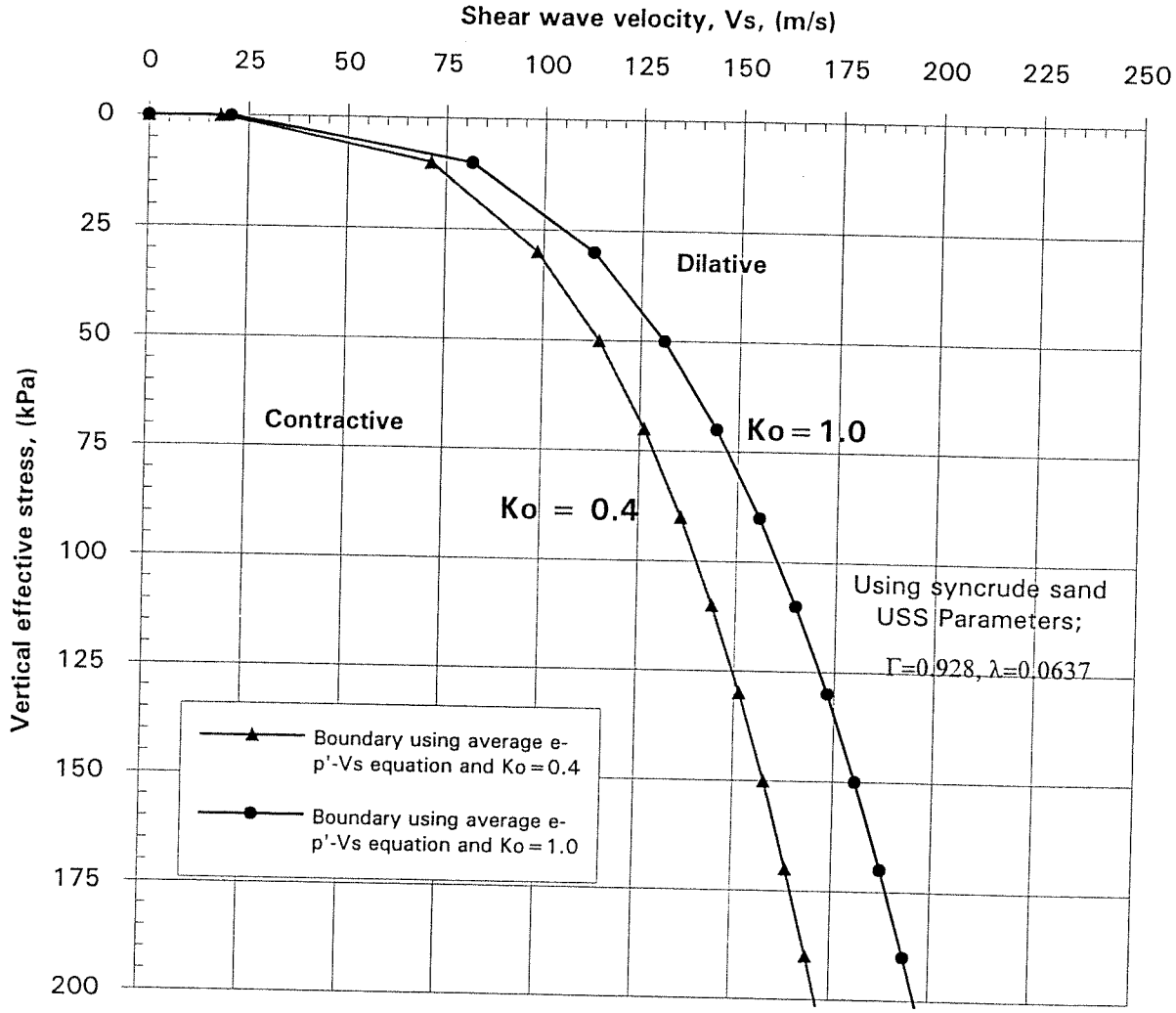

Figure 10. V_S versus σ'_v with contractive/dilative boundary ($\psi = 0$) for Syncrude sand for $K_o = 0.4$ and for $K_o = 1.0$.

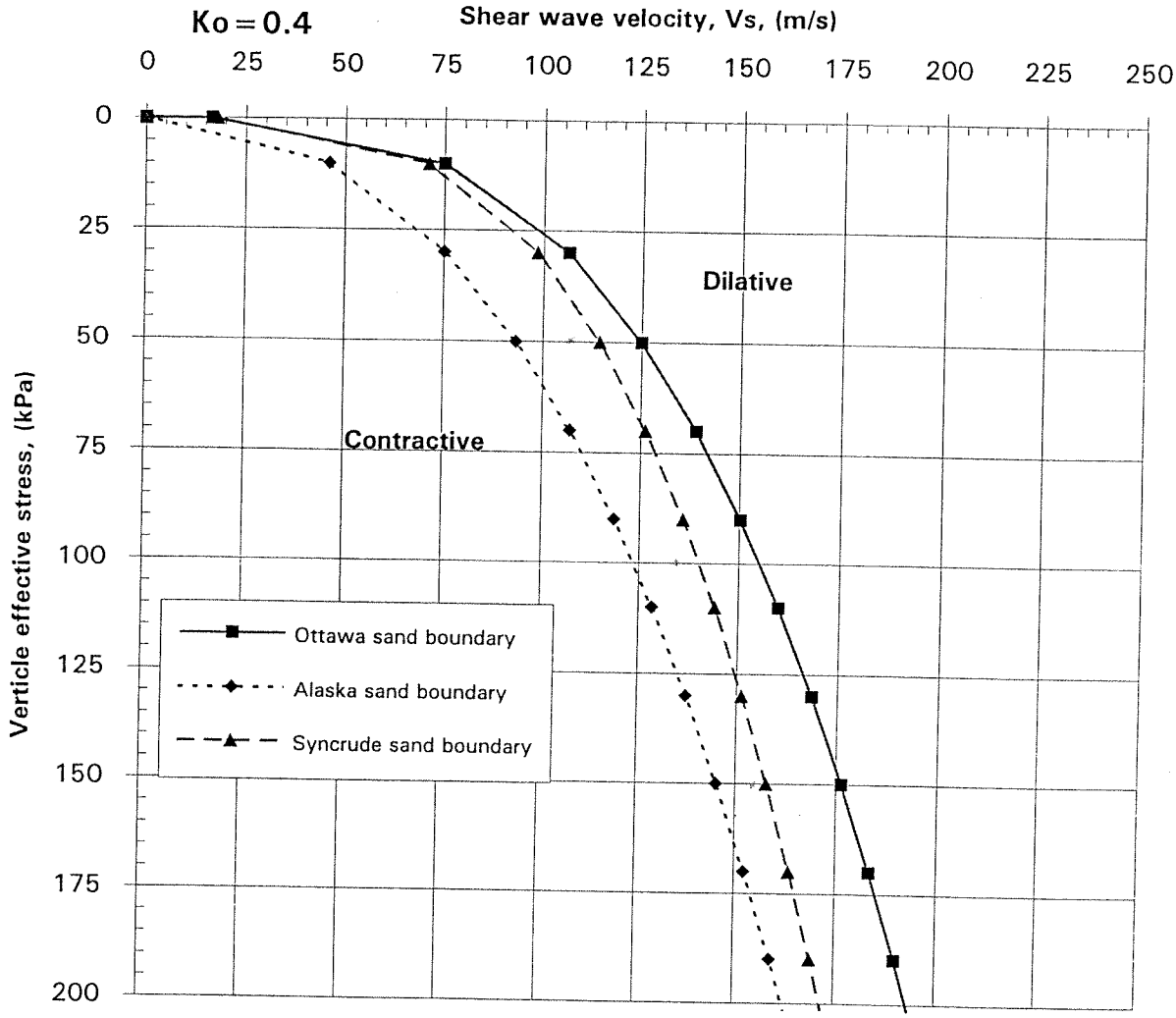

Figure 11. V_S versus σ'_v with contractive/dilative boundary ($\psi = 0$) for Ottawa, Alaska and Syncrude sands for $K_o = 0.4$.

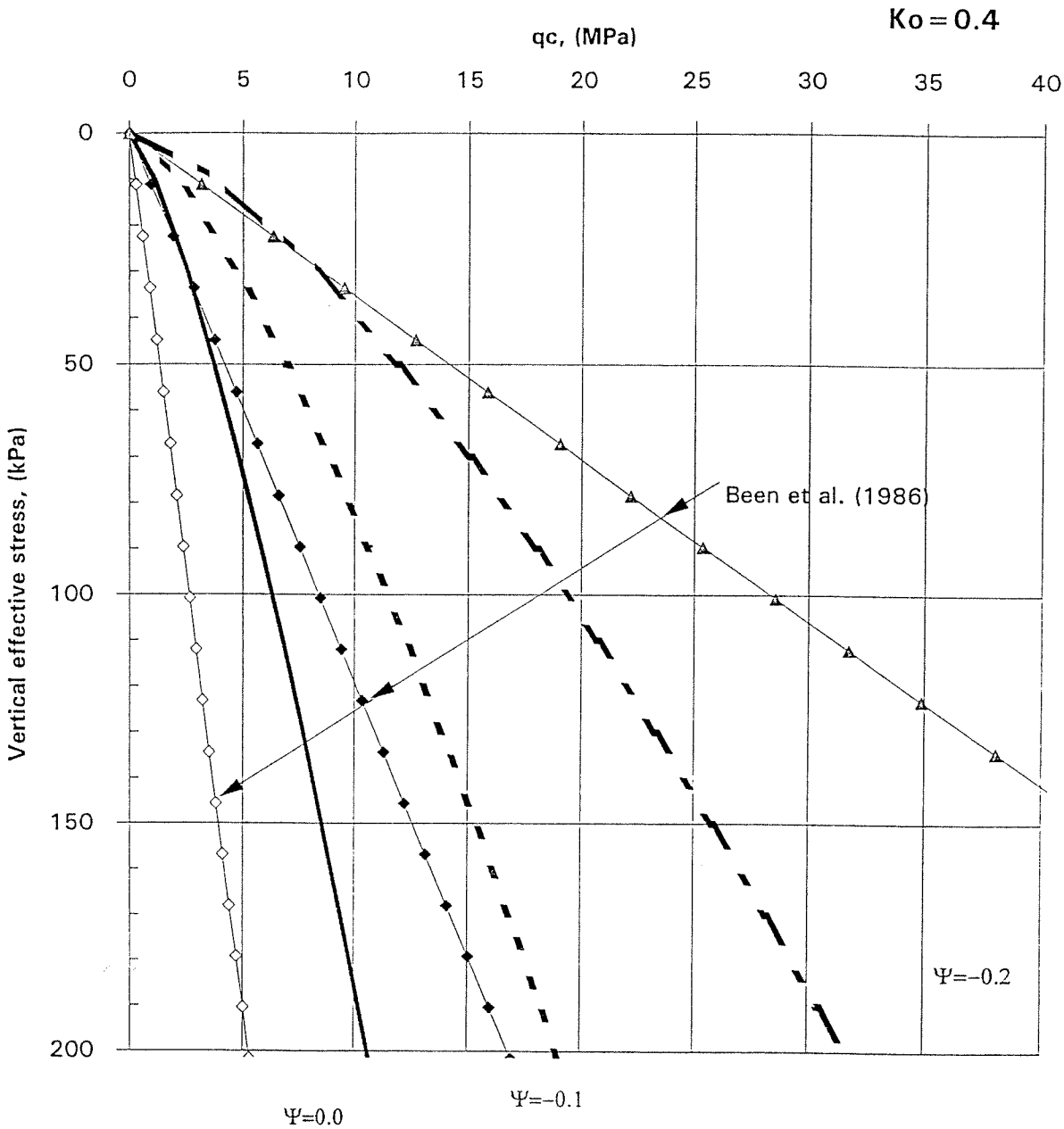

Figure 12. Comparison between contours of state parameter using cone penetration resistance, q_c, based on V_s correlation and method proposed by Been and Jefferies (1986) for Ottawa sand ($K_o = 0.4$).

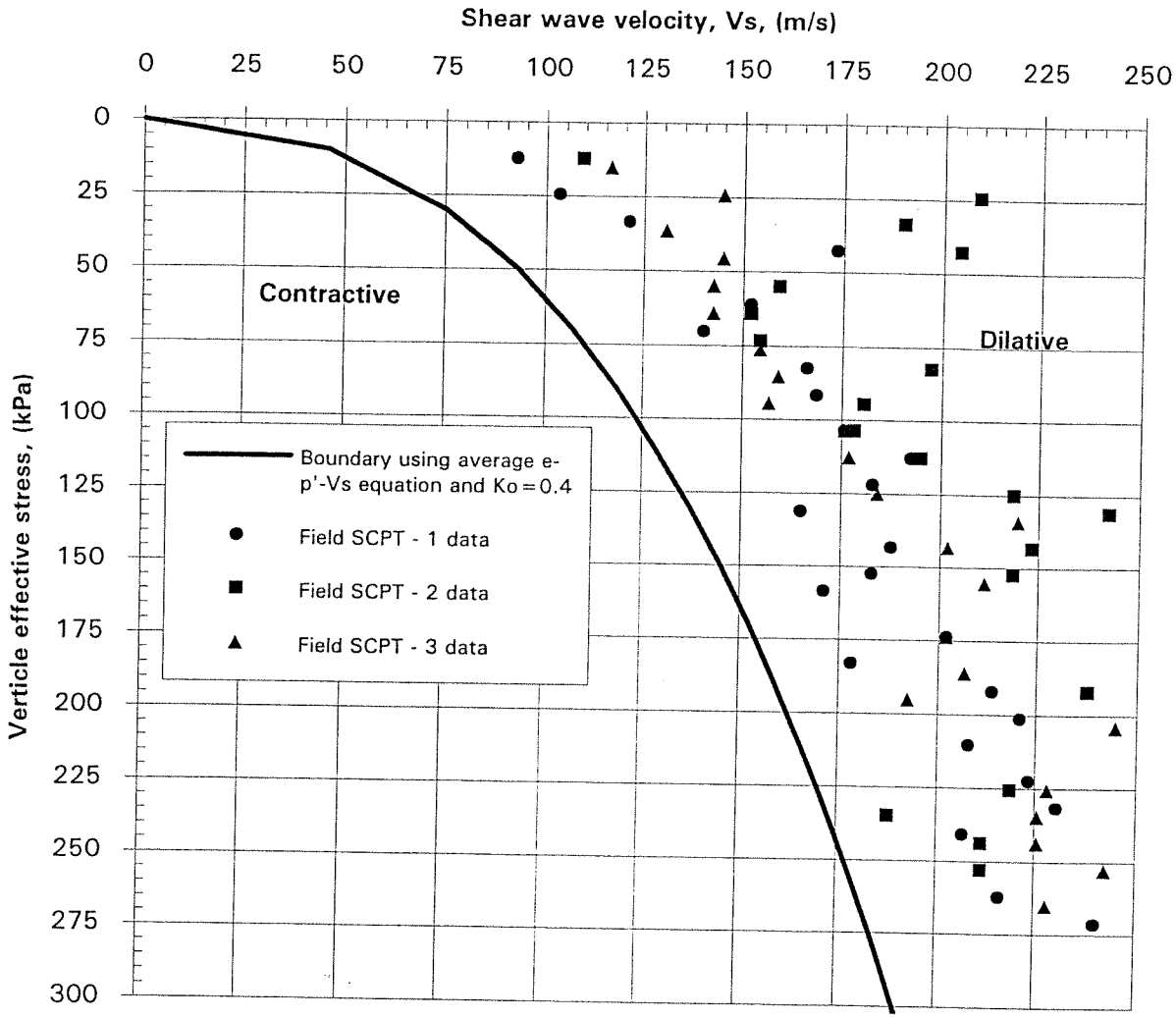

Figure 13. Alaska sand field data in terms of shear wave velocity compared to proposed contractive/dilative boundary.

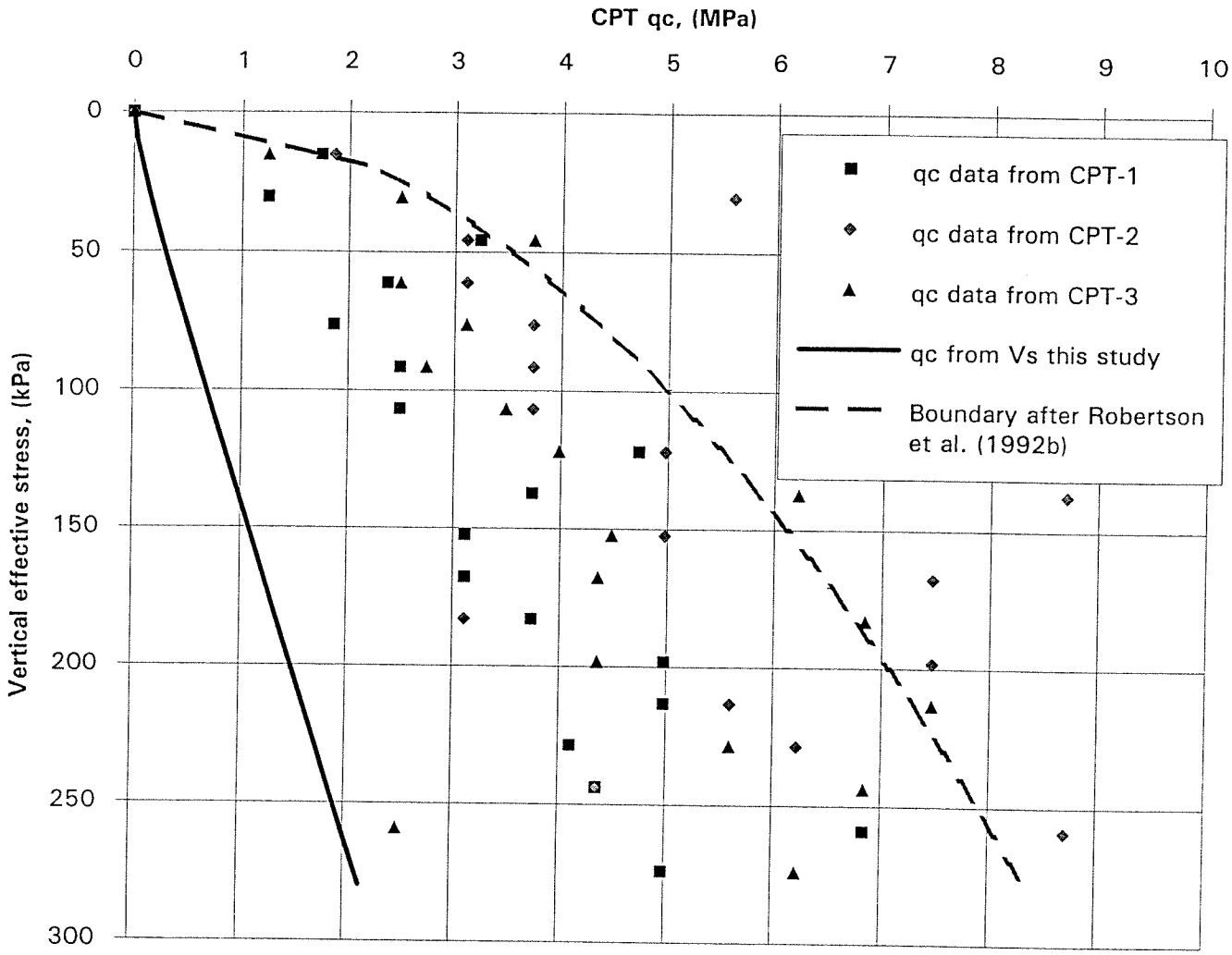

Figure 14. Alaska sand field CPT qc data versus σ'_v showing the contractive/dilative boundary determined in this study and that suggested by Robertson *et al.* (1992b) for an incompressible clean, silica sand.

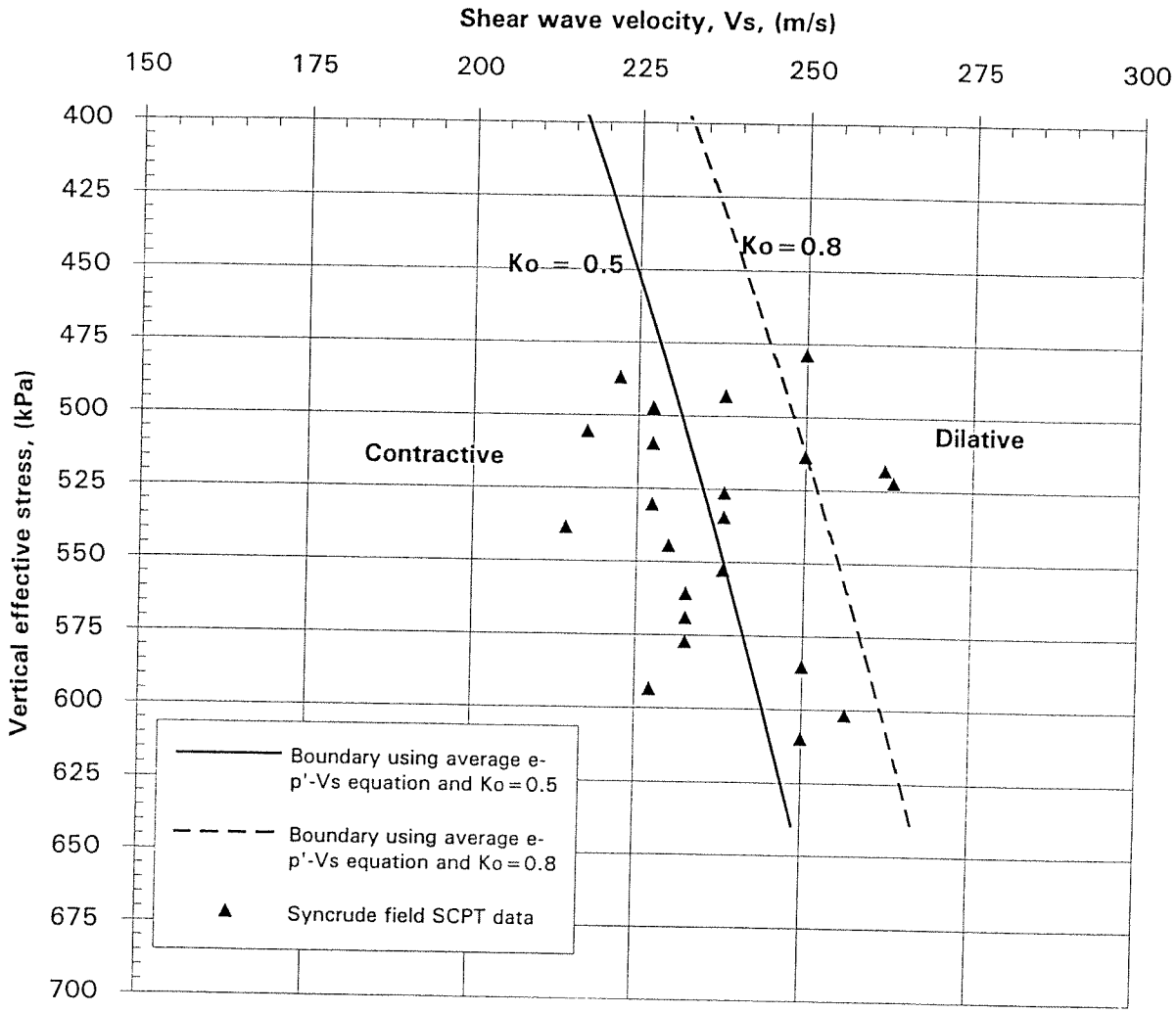

Figure 15. Syncrude sand field data in terms of shear wave velocity compared to proposed contractive/dilative boundary.